

1
2 **miR472 deficiency enhances *Arabidopsis thaliana* defence without reducing seed**
3 **production.**

4
5
6 Francois Vasseur^{1,2*}, Patricia Baldrich^{3,\$}, Tamara Jiménez-Góngora⁴, Luis Villar-Martin⁴,
7 Detlef Weigel² and Ignacio Rubio-Somoza^{2,4*}.
8

9 1 - CEFÉ, Univ Montpellier, CNRS, EPHE, IRD, Montpellier, France

10 2 - Department of Molecular Biology, Max Planck Institute for Biology Tübingen, Tübingen,
11 Germany.

12 3 - Centre for Research in Agricultural Genomics, Barcelona, Spain.

13 4 - Molecular Reprogramming and Evolution Laboratory. Centre for Research in Agricultural
14 Genomics, Barcelona, Spain.

15 -\$Present address: Donald Danforth Plant Science Centre, St. Louis, MO 63132.

16

17 *To whom correspondence should be addressed: Ignacio Rubio-Somoza
18 ignacio.rubio@craegenomica.es or francois.vasseur@cefe.cnrs.fr

19

20 **Abstract**

21 After having co-existed in plant genomes for at least 200 million years, the products of
22 microRNA (miRNA) and Nucleotide-Binding Leucine Rich Repeat protein (NLR) genes formed
23 a regulatory relationship in the common ancestor of modern gymnosperms and angiosperms.
24 From then on, DNA polymorphisms occurring at miRNA target sequences within NLR
25 transcripts must have been compensated by mutations in the corresponding mature miRNA
26 sequence, therefore maintaining that regulatory relationship. The potential evolutionary
27 advantage of such regulation remains largely unknown and might be related to two mutually
28 non-exclusive scenarios: miRNA-dependent regulation of NLR levels might prevent defence
29 mis-activation with negative effects on plant growth and reproduction; or reduction of active
30 miRNA levels in response to pathogen derived molecules (PAMPs and silencing suppressors)
31 might rapidly release otherwise silent NLR transcripts for rapid translation and thereby
32 enhance defence. Here, we used *Arabidopsis thaliana* plants deficient for miR472 function to
33 study the impact of releasing its NLR targets on plant growth and reproduction and on defence
34 against the fungal pathogen *Plectosphaeraella cucumerina*. We show that miR472 regulation
35 has a dual role, participating both in the tight regulation of plant defence and growth. MIM472
36 lines, with reduced active miR472, are more resistant to pathogens and, correlatively, have
37 reduced relative growth compared to wild-type plants. However, despite MIM472 lines flower
38 at the same time than their wild-type, the end of their reproductive phase is delayed, and they
39 exhibit higher adult biomass, resulting in similar seed yield as the wild-type. Our study
40 highlights how negative consequences of defence activation might be compensated by
41 changes in phenology and that miR472 reduction is an integral part of plant defence
42 responses.

43 **Introduction**

44 Pathogens are arguably one of the main threats to an organism's life. Accordingly, animals
45 and plants have developed sophisticated molecular mechanisms to perceive such threats and
46 defend themselves from invaders. Plants continuously monitor the potential presence of
47 pathogens with dedicated receptors at their cell surface. These proteins, named pattern
48 recognition receptors (PRR), detect molecular signatures conserved in broad classes of
49 microorganisms (DeFalco and Zipfel, 2021). In plants, PRR expression is often cell-type and
50 developmental-stage specific to match the most critical targets of infection (Beck et al., 2014,
51 Emonet et al., 2021). The patterns detected by PRRs refer to molecular signatures produced
52 by pathogens and dubbed pathogen- or microbe- associated molecular patterns
53 (PAMPs/MAMPs). Extracellular recognition of PAMPs by PRRs constitutes a first layer of
54 defence, PAMP-triggered immunity (PTI), which encompasses responses that modify the
55 host's defensive and developmental status, both at cellular and organismal levels (Bartels and
56 Boller, 2015).

57 A second surveillance system is dedicated to detecting the intracellular presence and action
58 of pathogen-derived molecules, effectors, used to manipulate the host for the pathogen's
59 benefit. This second layer of defence relies on proteins from the Nucleotide-binding site
60 leucine-rich repeat superfamily (NLR) (Adachi et al., 2019). NLRs also guard the regular
61 functioning of key host proteins that are hubs in fundamental cellular processes and that are
62 therefore often targets of pathogen intervention. Changes in these host guardees activate
63 NLRs, leading to Effector-Triggered Immunity (ETI) (Jones et al., 2016). While PTI and ETI
64 have initially been considered as independent arms of plant defence, they are now recognized
65 as being closely intertwined and sharing many signalling components, including the
66 participation of hormones such as salicylic (SA) and jasmonic acid (JA) (Lu and Tsuda, 2021).

67 Inappropriate activation of plant defences often leads to impairment of plant development,
68 growth, and fitness, in both natural settings and in controlled growth conditions (Zust and
69 Agrawal, 2017). Such defence-related trade-offs conform to the assumption that organisms
70 have limited resources to allocate to different physiological processes (Herms and Mattson,
71 1992). Thus, the increase of resources allocated to defence will result in a proportional
72 decrease in those available for other processes such as growth and/or reproduction. Over the
73 last decades, these trade-offs have been intensively investigated through different approaches
74 in a wide range of organisms (de Jong et al., 200, de Vries et al., 2017, Defossez et al., 2018,
75 Griffiths et al., 2018, Lind et al., 2013, Naseenn et al., 2015). Some studies have supported
76 their existence in plants (Karasov et al., 2014, Tian et al., 2003), although others have failed
77 to detect such trade-offs (Barto and Cipollini, 2005, McGuire and Agrawal, 2005).

78 To avoid inappropriate activation of defence, timing and magnitude of NLR-based responses
79 are under tight genetic control at the transcriptional, post-transcriptional, translational, and
80 post-translational levels (Cheng et al., 2011, Gloggnitzer et al., 2014, Lai and Eulgem, 2018,
81 Shao et al., 2019, Wu et al., 2017). NLR expression is controlled at the post-transcriptional
82 level by RNA decay and RNA silencing (Gloggnitzer et al., 2014, Shivaprasad et al., 2012,
83 Zhai et al., 2011). RNA silencing in turn relies on two classes of small RNAs (sRNAs); micro
84 RNAs (miRNAs) and small interfering RNAs (siRNAs). miRNAs have emerged as central
85 regulators of plant immunity by directly regulating the expression of NLR genes in a wealth of
86 plant species (Zhang et al., 2016). The impact of miRNA-mediated NLR regulation goes
87 beyond their direct targets, and amplification of the small RNA response serves to regulate

88 additional secondary NLR targets (Zhai et al., 2011). Such amplification starts with conversion
89 of primary targeted transcripts into double-stranded RNAs (dsRNAs) by RNA-dependent RNA
90 Polymerase 6 (RDR6) with 22 nucleotide long miRNAs as trigger. Subsequently, the dsRNAs
91 are recognized and processed by Dicer-Like 4 (DCL4), giving rise to phased secondary
92 siRNAs (phasiRNAs), which can target additional NLR transcripts based on sequence
93 complementarity. Attenuation of miRNA-mediated NLR suppression results in enhanced
94 resistance to viruses, bacteria, oomycetes and fungal pathogens in several plant species, such
95 as *Arabidopsis*, tomato and barley (Canto-Pastor et al., 2019, Liu et al., 2014, Lopez-Marquez
96 et al., 2021, Shivaprasad et al., 2012).

97 NLR proteins were already present in the common ancestor of the green lineage (Shao et al.,
98 2019), while miRNAs seem to have evolved independently in chlorophyte green and in brown
99 algae as well as in land plants (Tarver et al., 2015). The appearance of miRNAs targeting
100 NLRs can be traced back to the emergence of gymnosperms, although both miRNAs and
101 NLRs were already present in earlier land plants (Zhang et al., 2016). From that moment on,
102 miRNA-dependent NLR regulation have co-evolved. Different clades of NLR genes
103 themselves evolve at different speeds. Some clades rapidly expand through the generation of
104 NLR paralogs which in turn undergo frequent gene conversion. Other NLRs mainly evolve
105 through presence/absence polymorphisms. Rapidly evolving NLRs, which seem to be more
106 likely to be under miRNA regulation, have been proposed to be particularly beneficial in the
107 presence of new pathogen effectors, widening the resistance spectrum against pathogens
108 (Zhang et al., 2016). Likewise, new miRNA families appear to be continuously generated
109 throughout evolution, and at least eight independent miRNA families having been described
110 as NLR regulators in different groups of plants. Noteworthy, unrelated miRNAs converged to
111 target sequences that encode portions of the highly conserved and functional P-Loop protein
112 domain in their NLR targets. NLRs are under selection from highly dynamic pathogen threats,
113 hence, it has been suggested that NLRs are the driving force of this co-evolution by prompting
114 miRNA mutation and selection to, in turn, maintain their control on NLR expression (Zhang et
115 al., 2016).

116 Thus, two scenarios are possible. On the one hand, miRNAs have been evolutionary recruited
117 by the NLR networks to reduce collateral damage from inappropriate NLR activation. On the
118 other hand, miRNAs were added as a third layer to the pathogen response, with miRNAs
119 acting as indirect pathogen sensors.

120 We reasoned that if the role of NLR-regulating miRNAs is primarily to prevent undesired
121 developmental or physiological effects, plants lacking these miRNAs should also be
122 compromised in growth and reproduction. Alternatively, limited growth/reproduction defects
123 would favour a scenario in which miRNAs have a direct role in regulating defence.

124 The *A. thaliana* reference genome encodes two unrelated miRNAs that regulate NLR
125 expression, miR472 and miR825-5p (Boccara et al., 2014, Lopez-Marquez et al., 2021).
126 miR472 regulates a group of genes belonging to the coiled-coil-NLR (CC-NLR) sub-class,
127 while miR825-5p primarily targets members from the Toll-interleukin-receptor-like-NLR (TIR-
128 NLR) subfamily. Deficient miR472-mediated NLR regulation increases defence response
129 against the bacterial pathogen *Pseudomonas syringae* (Boccara et al., 2014).

130 Here, we have characterized the role of *A. thaliana* miR472-dependent NLR regulation in plant
131 defence against the fungal pathogen *Plectosphaeraella cucumerina* and its involvement in

132 different trade-offs. We report that miR472 downregulation is part of the response against
133 pathogens triggered by the detection of PAMPs produced by the hemibiotrophic fungus
134 *Plectosphaerella cucumerina*. Plants deficient in miR472 have lower rosette relative growth
135 rate (RGR) in the absence of pathogens, consistent with a growth-defence trade-off. However,
136 miR472 deficiency is also associated with a longer life cycle, leading to bigger size at
137 reproduction, and thus without a net effect on overall seed production.

138 **Results**

139 *Fungal PAMPs reduce miR472 levels*

140 Treatments with the bacterial PAMP flg22 downregulates *A. thaliana* miR472 (Boccara et al.,
141 2014, Su et al., 2018). Since we have also described a similar trend for some plant miRNAs
142 as part of fungal elicitor-triggered PTI, including the NLR-regulating miR825-5p (Lopez-
143 Marquez et al., 2021, Salvador-Guirao et al., 2018), we tested whether miR472 was also
144 responsive to fungal PAMPs. To that end, we measured the expression of miR472 and its
145 NLR target *At5g43740* after elicitor treatment. Four-week old wild-type Col-0 plants were
146 treated with either *P. cucumerina*-derived elicitors or with a mock solution, and samples were
147 collected at different time points. miR472 downregulation was readily detected as early as 30
148 minutes after elicitor treatment (Fig. 1A). Expressoin at later time points was variable, but
149 always lower than in control plants. Such a fluctuating expression pattern resembles the one
150 previously reported in response to flg22 (Boccara et al., 2014). The expression of At5g43740,
151 one of the miR472 target genes, did not increase until 60 minutes after elicitor treatment, and
152 its expression stayed elevated at later time points (Fig. 1B). These results are consistent with
153 miR472 acting through its target At5g43740 in the response to fungal elicitors.

154 *miRNA472 downregulation increases resistance to *Plectosphaerella cucumerina**

155 *Arabidopsis thaliana* plants deficient in miR472 can cope better with bacterial infections than
156 wild-type plants (Boccara, Sarazin et al. 2014). To assess whether miR472 deficiency also
157 contributes to increased resistance against fungal pathogens, we challenged miR472 target
158 mimic (MIM472) plants with reduced miR472 activity (Todesco, Rubio-Somoza et al. 2010)
159 with *P. cucumerina* (Petriacq, Stassen et al. 2016). MIM472 expression results in miR472
160 degradation and in higher levels of expression of at least one of its NLR targets, At5g43740
161 (Fig. 2A, Fig. S1). Four-week old MIM472 and control plants were inoculated with fungal
162 spores and plant survival was scored 12 days-post-inoculation (dpi). MIM472 plants
163 outperformed both wild-type and empty vector plants, with up to 70% survival, compared to
164 only around 30% of surviving control plants (Fig. 2B, C).

165 Prior to pathogen challenge, MIM472 plants did not show reduced photosynthetic capacity,
166 often a hallmark of defence responses (Berger et al., 2007, Rousseau et al., 2013) (Fig. S2).
167 Additionally,theseMIM472 plants did not present a correlation between increased resistance
168 (Fig. 2B, C) and the activation of hormone-mediated defence programs, as inferred from the
169 expression levels of marker genes for either JA- (*PDF1.2*, *VSP2*) or SA-dependent (*PR1*,
170 *PAD4*) pathways (Fig. S3). Together, these results show that miR472 regulates NLR targets
171 involved in anti-fungal defence and that its deficiency does not constitutively activate defence
172 markers.

173 Impaired *miRNA 472 activity decreases rosette relative growth rate (RGR)*

174 To evaluate a possible contribution from miR472 to NLR-dependent defence and
175 growth/fitness trade-offs, we monitored development, growth, and reproductive trajectories in
176 MIM472 and wild-type plants. Using the Raspberry Pi Automated Phenotyping Array (RAPA)
177 platform (Vasseur, Bresson et al. 2018) (Fig. 3A), we tracked rosette area in plants from two
178 MIM472 lines during ontogeny and until plant maturity (i.e., when fruits are ripening, which is
179 considered as the end of reproduction). Sigmoid growth curves were fitted on every individual
180 to estimate growth parameters (Fig. 3B). Rosette relative growth rate (RGR) was estimated
181 as the rate of increase in rosette area per unit existing area ($\text{mm}^2 \text{ d}^{-1} \text{ cm}^{-2}$) at the inflection
182 point of the growth curve (i.e. when absolute growth rate was maximal). The two MIM472 lines
183 had significantly lower RGR than Col-0 wild-type plants (Kruskal-Wallis $P < 0.05$; Fig. 4C), but
184 RGR reduction was not associated with a decrease of chlorophyll fluorescence, as inferred
185 from the F_v/F_m ratio measured on three-week old, unchallenged plants (Fig. S2). This ratio
186 reflects the efficiency of the photosystem to transport electrons (Bresson et al., 2015, Murchie
187 and Lawson, 2013), and it is often reduced with the onset of necrosis following pathogen attack
188 (Berger et al., 2007, Rousseau et al., 2013). Overall, these results point to a growth-defence
189 trade-off in plants with reduced miR472 activity. Moreover, the reduction of growth seems to
190 mainly result from an effect of miR472 on resource allocation rather than resource acquisition
191 through photosynthesis.

192 *Growth and phenological adjustments in MIM472 are associated with fitness homeostasis*

193 Despite significant differences in RGR, the timing of reproduction, measured as the age at
194 bolting, was similar between MIM472 lines and the wild-type Col-0 (Kruskal-Wallis $P > 0.05$
195 for MIM472-1, and $P = 0.02$ for MIM472-2; Fig. S3A). In contrast, we noticed that MIM472
196 individuals ended their reproduction two days later, on average, than Col-0 (Kruskal-Wallis P
197 < 0.01 ; Fig. 3D). Accordingly, MIM472 lines had longer reproductive phase than their wild-type
198 (Kruskal-Wallis $P < 0.01$ for MIM472-1, and $P = 0.11$ for MIM472-2; Fig. S3B). This prompted
199 us to test whether the coordinated changes in RGR and reproductive growth duration could
200 buffer the effects of defence-related processes on fitness in the MIM472 lines by determining
201 rosette dry mass at maturity (i.e., end of reproduction) as well as total seed yield (Fig. 4). Both
202 MIM472 lines had significantly higher rosette dry mass at maturity compared to Col-0 (Kruskal-
203 Wallis $P < 0.05$; Fig. 4B). By contrast, the seed yields of MIM472 and Col-0 wild-type plants
204 were not significantly different (Kruskal-Wallis $P > 0.05$; Fig. 4C), averaging at 60 mg of seeds
205 per plant for all genotypes, indicating that an extended growth phase compensates for slower
206 growth rate.

207 **Discussion**

208 It has been speculated that miRNA play an essential role to reduce the negative impact of
209 NLR expression on plant development (Gonzalez, Muller et al. 2015, Canto-Pastor, Santos et
210 al. 2019). Here, we characterized the phenotypic costs of higher NLR activity in mutants
211 impaired in miR472-dependent regulation. Our results are consistent with miRNA-dependent
212 regulation of defence is associated with few fitness costs in *Arabidopsis thaliana*. Likewise,
213 our results suggest that an advantage of miRNA-mediated NLR regulation allows for cell host
214 reprogramming upon detection of pathogen threats. Thus, pathogen-derived dysfunction of
215 host-proteins and sRNAs triggers NLR-mediated defence.

216 It is generally assumed that the metabolic cost of defence activation should be associated with
217 a concomitant decrease of growth and reproductive output (Herms and Mattson, 1992,

218 Karasov et al., 2017, Obeso, 2002). Indeed, resource allocation to growth and reproduction
219 are expected to be both negatively, and similarly, impacted by an increase in defence
220 metabolism. However, our results suggest that the relationships between growth,
221 reproduction, and defence are complex. We found that higher defence in MIM472 lines is
222 associated with slower relative growth rate but no reduction in seed production. Further
223 analysis showed that the slow-growing MIM472 lines have a longer life cycle, and specifically
224 a longer reproductive phase. Negative relationships between growth rate and lifespan are
225 commonly reported in large comparative studies among *A. thaliana* ecotypes (Debieu et al.,
226 2013, Sartori et al., 2019, Vasseur et al., 2014, Vasseur et al., 2018a), as well as among plant
227 species (Reich, 2014, Wright et al., 2004)). This is generally interpreted as the result of
228 physiological constraints, such as the necessity to allocate resources to structural compounds
229 to increase mechanical resistance and support a long lifespan. In *A. thaliana*, delayed
230 reproduction is associated with a higher accumulation of vegetative biomass. This increases
231 the availability of resources, such as nitrogen, to be possibly remobilized during senescence
232 from the vegetative to the reproductive parts (Killingbeck, 1996, Sartori et al., 2022).
233 Consistently, we found here that up-regulating defence can have a cost on relative growth
234 rate, as hypothesized by physiological considerations about the growth-defence trade-off,
235 while maintaining seed production. We argue that this maintenance of seed production is
236 reached by accumulating more vegetative biomass and extending reproduction to optimise
237 resource resorption from leaves to fruits. Together, our findings suggest that fitness can be
238 maintained upon defence activation through coordinated changes in plant physiology and
239 phenology.

240 Life history transitions such as the onset of flowering in annual plants are critical steps,
241 tightly regulated at the molecular level to integrate multiple environmental cues (Mouradov et
242 al., 2002). In *A. thaliana*, mechanisms that accelerate reproduction are expected to be
243 selected under water-limited conditions, for instance in Mediterranean regions where the
244 seasonal window with favourable water conditions is short (Vasseur et al., 2018b). Our
245 findings suggest that miRNA activity impacts plant development and phenology, which likely
246 interferes with the metabolic regulation triggered by environment signals such as temperature
247 and day length. Hence, if there is a fitness effect of defence activation in MIM472 lines, it is
248 not due to resource limitation for seed production, but rather on a potential mismatch between
249 environment and development. For instance, an inappropriate activation of defence might
250 delay reproduction and increase the risk of drought in Mediterranean climate. It is likely that
251 the physiological changes induced by the miRNA system of defence regulation might depend
252 on the number of NLR genes targeted and downregulated. Recent work has shown that
253 miRNAs mutate to keep on track with mutations in their targets (Zhang et al., 2016). We
254 propose here that this is not to prevent undesired effects on fitness, but rather to link their
255 upregulation to a failure of the silencing machinery as consequence of the presence of
256 pathogens, and thus, trigger a fast defence reprogramming to cope with those pathogen
257 threats. In line with that, reduction in functional miR472 and miR825-5p as consequence of
258 PAMP detection (this work, Boccaro et al., 2014, Lopez-Marquez et al., 2021) and/or the action
259 of silencing suppressors impinging sRNA function, which constitutes a conserved strategy
260 employed by different pathogens during infection (Csorba et al., 2015, Navarro et al., 2008,
261 Qiao et al., 2013, Zhu et al., 2022), are translated into enhanced NLR expression and defence.
262 Moreover, another reason for explaining conflicting findings about growth- and fitness-defence
263 trade-offs relies on the fact that most plant pathogens target vegetative tissues for infection

264 rather than reproductive organs. For instance, miR472, like miR825-5p, is preferentially
265 expressed in *Arabidopsis* leaves when compared to inflorescences (Vazquez et al., 2008),
266 which suggest that tissue and/or developmental stage restriction of miRNA-dependent
267 regulation of NLRs would aid to maximise defence response upon pathogen-triggered sRNA
268 dysfunction while minimising its effect on fitness. Further studies, for instance with reciprocal
269 transplants, are necessary to determine to what extent defence regulation by miRNAs might
270 have an environment-dependent cost on fitness, due to changes in life history rather than
271 changes in reproductive output.

272 **Conclusions**

273 Our study suggests that miRNAs targeting NLRs work to a large extent as sensors for the
274 presence of pathogens. sRNA-mediated NLR expression through miRNAs and amplifying
275 siRNAs render this system sensitive to silencing suppressors targeting many steps in both
276 regulatory pathways, such as those involved in miRNA biogenesis (DCL1, HYL1), miRNA
277 action (AGO1), and in siRNA amplification (RDR6, SGS3, DLC4, DRB4). Our results show
278 that the negative effect on growth from defence activation in MIM472 lines can be attenuated
279 by phenological adjustments leading to higher biomass and fitness homeostasis. Overall, this
280 suggests that growth-defence and fitness-defence trade-offs can be uncoupled due to
281 compensatory mechanisms involving different traits at different ontogenetic stages.

282

283

284 **Materials and Methods**

285 *Plant material*

286 MIM472 plants (Col-0 background) were produced and described in (Todesco, Rubio-Somoza
287 et al. 2010). For infection assays and elicitor treatments, Col-0 and MIM472 plants were grown
288 directly on a mixture of soil:perlite:vermiculine (2:1:1) under neutral day photoperiod (12h of
289 light and 12h of dark), at 22C during the day and 20C during the dark, and 60% relative
290 humidity, in controlled environments for four weeks for pathogen assays and until the end of
291 their life cycle for phenotyping assays.

292 *Infection assays and elicitor treatment*

293 *Plectosphaerella cucumerina* was grown at room temperature in petri dishes containing PDA
294 media (Potato Dextrose Agar, BD Difco), supplemented with chloramphenicol, for 3 weeks.
295 Spores were collected by adding sterile water to the surface of the plate, rubbing with a glass
296 cell spreader and collecting spores released in the water. Spore concentration was adjusted
297 to 1.10^6 using a Burker counting chamber and a light microscope. Spores were used to spray
298 inoculate six four weeks-old plants/genotype. The progression of the infection was monitored
299 up to 12 days after inoculation. For elicitor treatment, *Arabidopsis thaliana* Col-0 plants were
300 sprayed with an elicitor suspension obtained from *P. cucumerina* (300 μ g/ml) as previously
301 described (Coca and San Segundo 2010).

302

303 *Expression assays*

304 Total RNA was isolated using TRIzol reagent (Invitrogen). First-strand cDNA was synthesised
305 from 1 ug of TURBO DNase I (Ambion) or DNase I (Thermo Fisher) treated total RNA using
306 SuperScript III kit (Invitrogen) or Revertaid First strand kit (Thermo Fisher). Reverse
307 transcription quantitative PCR (RT-qPCR) was performed in a Light Cycler 480, using SYBR
308 green (Roche). Primers were designed using Oligo Analyzer software (Integrated DNA
309 Technologies).

310 For RT-qPCR, we used b-tubulin2 gene (At5g05620) as a housekeeping for transcript
311 expression normalisation. ΔCt method was used to analyse the results.

312 For miRNA expression, mature miR472 accumulation was determined by stem-loop RT-
313 qPCR, as described in (Varkonyi-Gasic, Wu et al. 2007). We confirmed the specific
314 amplification of the miR472 using amplicon sequencing.

315 For Northern blot assays, 20ug or total RNA were fractioned in a 17.5% polyacrylamide
316 denaturing gels containing 8 M urea and transferred to nylon membranes. Probes were design
317 to be complementary to miR472 and end-labelled with γ 32P-ATP.

318 All primers and probes used in this study are indicated in supplemental table 1.

319

320 *Phenotyping of growth- and fitness-related traits*

321 Seeds of Col-0, MIM472 #1 and MIM472 #2 were sown in individual pots ($n = 10$), randomly
322 distributed in trays of 30 pots each. Circular pots of 4.6 cm (diameter) x 5 cm (depth)
323 (Pöppelmann, Lohne, Germany) were filled with soil (CL T Topferde; www.einheitserde.de).
324 After germination, plants were thinned to one individual per pot, and trays were moved to the
325 Raspberry Pi Automated Plant Analysis (RAPA) facility (Vasseur et al., Plant Methods 2018),
326 set to 16°C, air humidity at 65%, and 12 h day length, with a PPFD of 125 to 175 μ mol m-2 s-
327 1 provided by a 1:1 mixture of Cool White and Gro-Lux Wide Spectrum fluorescent lights
328 (Luxline plus F36W/840, Sylvania, Germany). Trays were randomly positioned in the room
329 and watered every 2 to 4 days.

330 Growth-related traits were measured using methodologies previously published (Vasseur,
331 Bresson et al. 2018). The RAPA system was used for rosette imaging during the first 28 days
332 of growth. Rosette area (cm^2) was measured from pictures with imageJ (Schneider, Rasband
333 et al. 2012). Sigmoid growth curves were fitted on all individuals as previously described
334 (Vasseur, Bresson et al. 2018). From the parameters of the fitted functions, we estimated RGR
335 (rosette growth rate at time t divided by rosette area at time t , $\text{mm}^2 \text{d}^{-1} \text{cm}^{-2}$) over time. We
336 used RGR at the inflection point of the growth curve from each individual for comparison,
337 which corresponds to the transition point between the vegetative and the reproductive phases,
338 when the absolute growth rate is maximal. We used the inflection point as estimates of bolting
339 stage (in days). We estimated the efficiency of photosynthesis with images of chlorophyll
340 fluorescence, measured with F_v/F_m ratio at the whole-plant level, after 20 min of dark-
341 adaptation on three-week old rosettes. Chlorophyll fluorescence images were taken with a
342 high-throughput imaging system (Imaging-PAM M-Series, Maxi-version, Heinz Walz GmbH,
343 Germany), and analysed with ImageJ (Schneider, Rasband et al. 2012) to estimate mean
344 F_v/F_m of each rosette individually (Bresson, Vasseur et al. 2015) for details about chlorophyll
345 fluorescence measurements).

346 Plants were harvested at maturity, when fruits were ripening. Age at maturity (d) was
347 measured as the duration between germination and the end of reproduction. Rosettes were
348 separated from reproductive parts, photographed with a high-resolution, 16.6 megapixel SLR

349 camera (Canon EOS-1, Canon Inc., Japan), then dried at 65° C for three days and weighed
350 to measure rosette dry mass (DM, mg). Inflorescences were dried at 35 °C for one week in
351 paper bags. Seeds were collected and sifted to remove shoot fragments and weighed.

352 *Statistical analyses*

353 Statistical significance from expression assays (RT-qPCR) was determined using an ANOVA
354 test adjusted (p<0,05).

355 For phenotypic analysis, logistic functions were fitted with *nls* in R. Differences in phenotypic
356 traits between Col-0 and the two MIM472 lines were tested with non-parametric Kruskal-Wallis
357 tests. All statistical analyses were performed in R v3.2.3.

358

359 **Acknowledgements**

360 We would like to thank Miguel Angel Blazquez, Pere Puigdomenech and members of the
361 MoRE Lab for critical reading of the manuscript. Work at the Max Planck Institute was funded
362 by the Max Planck Society (D.W.). The work in the MoRE laboratory is funded by BFU-2014-
363 58361-JIN (funded by MCIN/AEI/ 10.13039/501100011033 and by “ESF Investing in your
364 future”), RYC-2015-19154 (funded by MCIN/AEI/ 10.13039/501100011033 and by “ESF
365 Investing in your future”), RTI2018-097262-B-I00 (funded by MCIN/AEI/
366 10.13039/501100011033 and by “ERDF A way of making Europe”); and through the “Severo
367 Ochoa Programme for Centres of Excellence in R&D” 2016-2019 (SEV-2015-0533) and 2020-
368 2023 (CEX2019-000902-S) funded by MCIN/AEI/ 10.13039/501100011033 and the CERCA
369 programme from the Generalitat de Catalunya. L. V-M was supported by BES-2016-076986
370 (funded by MCIN/AEI/ 10.13039/501100011033 and by “ESF Investing in your future”).
371 Tamara Jiménez-Góngora was recipient of a Postdoctoral Fellowship from the CRAG through
372 the “Severo Ochoa Programme for Centres of Excellence in R&D” 2016-2019 (SEV-2015-
373 0533).

374

375 **Figure legends**

376 **Figure 1. Fungal elicitors trigger a downregulation of miR472 and up-regulation of its
377 target in *Arabidopsis thaliana*.**

378 **A.** Accumulation of miR472 determined by small RNA Northern blot in a time course of wild-
379 type Col-0 plants treated with *P. cucumerina* elicitors (300 µg/ml), or mock solution (control).
380 Northern blots were hybridized with a γ 32P-ATP end-labelled probe complementary to
381 miR472. Ribosomal RNA (rRNA) was used as a loading control. Relative band density was
382 determined using ImageJ and normalized to the intensity of its corresponding rRNA control
383 and, subsequently, to the corresponding control time point.

384 **B.** Relative expression of miR472 target CC-NBS-LRR (At5g43740), as determined by reverse
385 transcription quantitative PCR (RT-qPCR). The β -tubulin2 gene (At5g05620) was used as
386 housekeeping for transcript expression normalization. The experiment was repeated for a total
387 of three biological replicates. All replicates presented similar results. The histogram shows
388 results of one of the three biological replicates.

389 **Figure 2. MIM472 plants are more resistant to *P. cucumerina* infection.**

390 **A.** Relative expression of a miR472 CC-NBS-LRR target (At5g43740), as determined by RT-
391 qPCR. The β -tubulin2 gene (At5g05620) was used as a housekeeping gene for transcript
392 expression normalization. Three biological and technical replicates were included in the assay.
393 Significance codes (ANOVA-test): *: $p < 0.05$.

394 **B.** Plants 12 days after spray-inoculation with *P. cucumerina* spores (1.10^6 spores/ml). Six
395 biological replicates were used for each genotype. All biological replicates behaved similarly.
396 Histogram shows results from one of the three biological replicates.

397 **C.** Survival ratio of plants infected with *P. cucumerina* spores (1.10^6 spores/ml) at 12 days
398 post infection. Six biological replicates were used for each genotype. All technical replicates
399 behaved similarly, showing results of one of the three technical replicates.

400

401 **Figure 3. Variation of growth and phenology in MIM472 lines.**

402 **A.** Photography of the Raspberry Pi Automated Phenotyping Array (RAPA) phenotyping
403 platform, with trays of *Arabidopsis thaliana* grown in highly controlled conditions

404 **B.** Growth curves of two MIM472 lines (MIM472 #1 in red and MIM472 #2 in orange) and the
405 wild-type Col-0 (in blue) grown in RAPA ($n = 10$). Dots are the rosette area (cm^2) measured
406 from image analysis, with the last ones measured at maturity when plants were harvested.
407 Curves were fitted with logistic models. At the top of the graph is a representative rosette (Col-
408 0) with images taken during ontogeny.

409 **C.** Differences in relative growth rate (RGR) between the two MIM472 lines and the wild-type
410 Col-0 ($n = 10$).

411 **D.** Differences in age at bolting between the two MIM472 lines and the wild-type Col-0 ($n =$
412 10). (C) Differences in age at maturity between the two MIM472 lines and the wild-type Col-0
413 ($n = 10$). Significance codes (Kruskal-Wallis non-parametric tests): ***: $p < 0.001$; **: $p < 0.01$;
414 *: $p < 0.05$; NS: $p > 0.05$.

415 **Figure 4. Variation of rosette dry mass and seed yield in MIM472 lines.**

416 **A.** Examples of pictures taken at maturity (end of reproduction).

417 **B.** Differences in rosette dry mass (DM, mg) between the two MIM472 lines and the wild-type
418 Col-0 ($n = 10$).

419 **C.** Differences in total seed yield (mg) between the two MIM472 lines and the wild-type Col-0
420 ($n = 10$). Significance codes (Kruskal-Wallis non-parametric tests): ***: $p < 0.001$; **: $p < 0.01$;
421 *: $p < 0.05$; NS: $p > 0.05$.

422 **Supplemental Figure 1. MIM472 plants show lower levels of mature miR472.**

423 Validation of lower levels of mature miR472 in MIM472 plants compared to WT by RT-qPCR.
424 As described in (Todesco, Rubio-Somoza et al. 2010) functional MIM constructs trigger
425 degradation of the decoyed miRNA resulting in lower levels of its mature form. Two biological

426 and technical replicates were included in RT-qPCR assays. Significance codes (ANOVA-test):
427 *: $p < 0.05$.

428 **Supplemental Figure 2. Variation of photosynthesis efficiency in MIM472 lines.**

429 Photosynthesis efficiency was measured with chlorophyll fluorescence (Fv/Fm ratio, unitless)
430 on three-week old plants ($n = 10$). Pictures used as examples here were coloured with imageJ.
431 Significance codes (Kruskal-Wallis non-parametric tests): ***: $p < 0.001$; **: $p < 0.01$; *: $p <$
432 0.05 ; NS: $p > 0.05$.

433 **Supplemental Figure 3. Expression pattern of defence-related hormone marker genes.**

434 **A.** Expression analysis of the SA marker gene PR1 by RT-qPCR in MIM472 and WT plants.

435 **B.** Expression analysis of the SA marker gene PAD4 by RT-qPCR in MIM472 and WT plants.

436 **C.** Expression analysis of the JA marker gene PDF1.2 by RT-qPCR in MIM472 and WT plants.

437 **D.** Expression analysis of the JA marker gene VSP2 by RT-qPCR in MIM472 and WT plants.

438 Two biological and technical replicates were included in RT-qPCR assays. Significance codes
439 (ANOVA-test): *: $p < 0.05$.

440

441 **REFERENCES**

442

443 ADACHI, H., DEREVNINA, L. & KAMOUN, S. 2019. NLR singletons, pairs, and networks:
444 evolution, assembly, and regulation of the intracellular immunoreceptor circuitry of
445 plants. *Curr Opin Plant Biol*, 50, 121-131.

446 BARTELS, S. & BOLLER, T. 2015. Quo vadis, Pep? Plant elicitor peptides at the crossroads
447 of immunity, stress, and development. *J Exp Bot*, 66, 5183-93.

448 BARTO, E. K. & CIPOLLINI, D. 2005. Testing the optimal defense theory and the growth-
449 differentiation balance hypothesis in *Arabidopsis thaliana*. *Oecologia*, 146, 169-178.

450 BECK, M., WYRSCH, I., STRUTT, J., WIMALASEKERA, R., WEBB, A., BOLLER, T. &
451 ROBATZEK, S. 2014. Expression patterns of flagellin sensing 2 map to bacterial
452 entry sites in plant shoots and roots. *J Exp Bot*, 65, 6487-98.

453 BERGER, S., SINHA, A. K. & ROITSCH, T. 2007. Plant physiology meets phytopathology:
454 plant primary metabolism and plant-pathogen interactions. *Journal of Experimental
455 Botany*, 58, 4019-4026.

456 BOCCARA, M., SARAZIN, A., THIEBEAULD, O., JAY, F., VOINNET, O., NAVARRO, L. &
457 COLOT, V. 2014. The *Arabidopsis* miR472-RDR6 silencing pathway modulates
458 PAMP- and effector-triggered immunity through the post-transcriptional control of
459 disease resistance genes. *PLoS Pathog*, 10, e1003883.

460 BRESSON, J., VASSEUR, F., DAUZAT, M., KOCH, G., GRANIER, C. & VILE, D. 2015.
461 Quantifying spatial heterogeneity of chlorophyll fluorescence during plant growth and
462 in response to water stress. *Plant Methods*, 11.

463 CANTO-PASTOR, A., SANTOS, B., VALLI, A. A., SUMMERS, W., SCHORNACK, S. &
464 BAULCOMBE, D. C. 2019. Enhanced resistance to bacterial and oomycete
465 pathogens by short tandem target mimic RNAs in tomato. *Proc Natl Acad Sci U S A*,
466 116, 2755-2760.

467 CHENG, Y. T., LI, Y., HUANG, S., HUANG, Y., DONG, X., ZHANG, Y. & LI, X. 2011.
468 Stability of plant immune-receptor resistance proteins is controlled by SKP1-

469 CULLIN1-F-box (SCF)-mediated protein degradation. *Proc Natl Acad Sci U S A*, 108,
470 14694-9.

471 CSORBA, T., KONTRA, L. & BURGYAN, J. 2015. viral silencing suppressors: Tools forged
472 to fine-tune host-pathogen coexistence. *Virology*, 479-480, 85-103.

473 DE JONG, T. J., & VAN DER MEIJDEN, E. (2000). On the Correlation between Allocation to
474 Defence and Regrowth in Plants. *Oikos*, 88, 503–508.

475 DE VRIES, J., EVERE, J. B. & POELMAN, E. H. 2017. Dynamic Plant-Plant-Herbivore
476 Interactions Govern Plant Growth-Defence Integration. *Trends Plant Sci*, 22, 329-
477 337.

478 DEBIEU, M., TANG, C., STICH, B., SIKOSEK, T., EFFGEN, S., JOSEPHS, E., SCHMITT,
479 J., NORDBORG, M., KOORNNEEF, M. & DE MEAUX, J. 2013. Co-Variation
480 between Seed Dormancy, Growth Rate and Flowering Time Changes with Latitude in
481 *Arabidopsis thaliana*. *Plos One*, 8.

482 DEFALCO, T. A. & ZIPFEL, C. 2021. Molecular mechanisms of early plant pattern-triggered
483 immune signaling. *Mol Cell*, 81, 4346.

484 DEFOSSEZ, E., PELLISSIER, L. & RASMANN, S. 2018. The unfolding of plant growth form-
485 defence syndromes along elevation gradients. *Ecology Letters*, 21, 609-618.

486 EMONET, A., ZHOU, F., VACHERON, J., HEIMAN, C. M., DENERVAUD TENDON, V., MA,
487 K. W., SCHULZE-LEFERT, P., KEEL, C. & GELDNER, N. 2021. Spatially Restricted
488 Immune Responses Are Required for Maintaining Root Meristematic Activity upon
489 Detection of Bacteria. *Curr Biol*, 31, 1012-1028 e7.

490 GLOGGNITZER, J., AKIMCHEVA, S., SRINIVASAN, A., KUSENDA, B., RIEHS, N.,
491 STAMPFL, H., BAUTOR, J., DEKROUT, B., JONAK, C., JIMENEZ-GOMEZ, J. M.,
492 PARKER, J. E. & RIHA, K. 2014. Nonsense-mediated mRNA decay modulates
493 immune receptor levels to regulate plant antibacterial defense. *Cell Host Microbe*, 16,
494 376-90.

495 GRIFFITHS, J. I., PETCHEY, O. L., PENNEKAMP, F. & CHILDS, D. Z. 2018. Linking
496 intraspecific trait variation to community abundance dynamics improves ecological
497 predictability by revealing a growth-defence trade-off. *Functional Ecology*, 32, 496-
498 508.

499 HERMS, D. A. & MATTSON, W. J. 1992. The Dilemma of Plants - to Grow or Defend (Q Rev
500 Biol, Vol 67, Pg 283, 1992). *Quarterly Review of Biology*, 67, 478-478.

501 JONES, J. D., VANCE, R. E. & DANGL, J. L. 2016. Intracellular innate immune surveillance
502 devices in plants and animals. *Science*, 354.

503 KARASOV, T. L., CHAE, E., HERMAN, J. J. & BERGELSON, J. 2017. Mechanisms to
504 Mitigate the Trade-Off between Growth and Defense. *Plant Cell*, 29, 666-680.

505 KARASOV, T. L., KNISKERN, J. M., GAO, L., DEYOUNG, B. J., DING, J., DUBIELLA, U.,
506 LASTRA, R. O., NALLU, S., ROUX, F., INNES, R. W., BARRETT, L. G., HUDSON,
507 R. R. & BERGELSON, J. 2014. The long-term maintenance of a resistance
508 polymorphism through diffuse interactions. *Nature*, 512, 436-440.

509 KILLINGBECK, K. T. 1996. Nutrients in senesced leaves: Keys to the search for potential
510 resorption and resorption proficiency. *Ecology*, 77, 1716-1727.

511 LAI, Y. & EULGEM, T. 2018. Transcript-level expression control of plant NLR genes. *Mol
512 Plant Pathol*, 19, 1267-1281.

513 LIND, E. M., BORER, E., SEABLOOM, E., ADLER, P., BAKKER, J. D., BLUMENTHAL, D.
514 M., CRAWLEY, M., DAVIES, K., FIRN, J., GRUNER, D. S., HARPOLE, W. S.,
515 HAUTIER, Y., HILLEBRAND, H., KNOPS, J., MELBOURNE, B., MORTENSEN, B.,
516 RISCH, A. C., SCHUETZ, M., STEVENS, C. & WRAGG, P. D. 2013. Life-history
517 constraints in grassland plant species: a growth-defence trade-off is the norm.
518 *Ecology Letters*, 16, 513-521.

519 LIU, J., CHENG, X., LIU, D., XU, W., WISE, R. & SHEN, Q. H. 2014. The miR9863 family
520 regulates distinct Mla alleles in barley to attenuate NLR receptor-triggered disease
521 resistance and cell-death signaling. *PLoS Genet*, 10, e1004755.

522 LOPEZ-MARQUEZ, D., DEL-ESPINO, A., LOPEZ-PAGAN, N., RODRIGUEZ-NEGRENTE, E.
523 A., RUBIO-SOMOZA, I., RUIZ-ALBERT, J., BEJARANO, E. R. & BEUZON, C. R.

524 2021. miR825-5p targets the TIR-NBS-LRR gene MIST1 and down-regulates basal
525 immunity against *Pseudomonas syringae* in *Arabidopsis*. *J Exp Bot*, 72, 7316-7334.

526 LU, Y. & TSUDA, K. 2021. Intimate Association of PRR- and NLR-Mediated Signaling in
527 Plant Immunity. *Mol Plant Microbe Interact*, 34, 3-14.

528 MCGUIRE, R. & AGRAWAL, A. A. 2005. Trade-offs between the shade-avoidance response
529 and plant resistance to herbivores? Tests with mutant *Cucumis sativus*. *Functional
530 Ecology*, 19, 1025-1031.

531 MOURADOV, A., CREMER, F. & COUPLAND, G. 2002. Control of flowering time:
532 Interacting pathways as a basis for diversity. *Plant Cell*, 14, S111-S130.

533 MURCHIE, E. H. & LAWSON, T. 2013. Chlorophyll fluorescence analysis: a guide to good
534 practice and understanding some new applications. *Journal of Experimental Botany*,
535 64, 3983-3998.

536 NASEENN, M., KALTDORF, M. & DANDEKAR, T. 2015. The nexus between growth and
537 defence signalling: auxin and cytokinin modulate plant immune response pathways.
538 *Journal of Experimental Botany*, 66, 4885-4896.

539 NAVARRO, L., JAY, F., NOMURA, K., HE, S. Y. & VOINNET, O. 2008. Suppression of the
540 microRNA pathway by bacterial effector proteins. *Science*, 321, 964-7.

541 OBESO, J. R. 2002. The costs of reproduction in plants. *New Phytologist*, 155, 321-348.

542 QIAO, Y., LIU, L., XIONG, Q., FLORES, C., WONG, J., SHI, J., WANG, X., LIU, X., XIANG,
543 Q., JIANG, S., ZHANG, F., WANG, Y., JUDELSON, H. S., CHEN, X. & MA, W. 2013.
544 Oomycete pathogens encode RNA silencing suppressors. *Nat Genet*, 45, 330-3.

545 REICH, P. B. 2014. The world-wide 'fast-slow' plant economics spectrum: a traits manifesto.
546 *Journal of Ecology*, 102, 275-301.

547 ROUSSEAU, C., BELIN, E., BOVE, E., ROUSSEAU, D., FABRE, F., BERRUYER, R.,
548 GUILLAUMES, J., MANCEAU, C., JACQUES, M. A. & BOUREAU, T. 2013. High
549 throughput quantitative phenotyping of plant resistance using chlorophyll
550 fluorescence image analysis. *Plant Methods*, 9.

551 SALVADOR-GUIRAO, R., BALDRICH, P., WEIGEL, D., RUBIO-SOMOZA, I. & SAN
552 SEGUNDO, B. 2018. The MicroRNA miR773 Is Involved in the *Arabidopsis* Immune
553 Response to Fungal Pathogens. *Mol Plant Microbe Interact*, 31, 249-259.

554 SARTORI, K., VASSEUR, F., VIOILLE, C., BARON, E., GERARD, M., ROWE, N., AYALA-
555 GARAY, O., CHRISTOPHE, A., DE JALON, L. G., MASCLEF, D., HARSCOUE, E.,
556 GRANADO, M. D., CHASSAGNEUX, A., KAZAKOU, E. & VILE, D. 2019. Leaf
557 economics and slow-fast adaptation across the geographic range of *Arabidopsis
558 thaliana*. *Scientific Reports*, 9.

559 SARTORI, K., VIOILLE, C., VILE, D., VASSEUR, F., VILLEMERREUIL, P., BRESSON, J.,
560 GILLESPIE, L., FLETCHER, L. R., SACK, L. & KAZAKOU, E. 2022. Do leaf nitrogen
561 resorption dynamics align with the slow-fast continuum? A test at the intraspecific
562 level. *Functional Ecology*, 36, 1315-1328.

563 SHAO, Z. Q., XUE, J. Y., WANG, Q., WANG, B. & CHEN, J. Q. 2019. Revisiting the Origin
564 of Plant NBS-LRR Genes. *Trends Plant Sci*, 24, 9-12.

565 SHIVAPRASAD, P. V., CHEN, H. M., PATEL, K., BOND, D. M., SANTOS, B. A. &
566 BAULCOMBE, D. C. 2012. A microRNA superfamily regulates nucleotide binding
567 site-leucine-rich repeats and other mRNAs. *Plant Cell*, 24, 859-74.

568 SU, Y., LI, H. G., WANG, Y., LI, S., WANG, H. L., YU, L., HE, F., YANG, Y., FENG, C. H.,
569 SHUAI, P., LIU, C., YIN, W. & XIA, X. 2018. Poplar miR472a targeting NBS-LRRs is
570 involved in effective defence against the necrotrophic fungus *Cytospora
571 chrysosperma*. *J Exp Bot*, 69, 5519-5530.

572 TARVER, J. E., CORMIER, A., PINZON, N., TAYLOR, R. S., CARRE, W., STRITTMATTER,
573 M., SEITZ, H., COELHO, S. M. & COCK, J. M. 2015. microRNAs and the evolution of
574 complex multicellularity: identification of a large, diverse complement of microRNAs
575 in the brown alga *Ectocarpus*. *Nucleic Acids Res*, 43, 6384-98.

576 TIAN, D., TRAW, M. B., CHEN, J. Q., KREITMAN, M. & BERGELSON, J. 2003. Fitness
577 costs of R-gene-mediated resistance in *Arabidopsis thaliana*. *Nature*, 423, 74-7.

578 VASSEUR, F., BONTPART, T., DAUZAT, M., GRANIER, C. & VILE, D. 2014. Multivariate
579 genetic analysis of plant responses to water deficit and high temperature revealed
580 contrasting adaptive strategies. *Journal of Experimental Botany*, 65, 6457-6469.

581 VASSEUR, F., EXPOSITO-ALONSO, M., AYALA-GARAY, O. J., WANG, G., ENQUIST, B.
582 J., VILE, D., VIOLLE, C. & WEIGEL, D. 2018a. Adaptive diversification of growth
583 allometry in the plant *Arabidopsis thaliana*. *Proceedings of the National Academy of
584 Sciences of the United States of America*, 115, 3416-3421.

585 VASSEUR, F., SARTORI, K., BARON, E., FORT, F., KAZAKOU, E., SEGRESTIN, J.,
586 GARNIER, E., VILE, D. & VIOLLE, C. 2018b. Climate as a driver of adaptive
587 variations in ecological strategies in *Arabidopsis thaliana*. *Annals of Botany*, 122,
588 935-945.

589 VAZQUEZ, F., BLEVINS, T., AILHAS, J., BOLLER, T. & MEINS, F., JR. 2008. Evolution of
590 *Arabidopsis* MIR genes generates novel microRNA classes. *Nucleic Acids Res*, 36,
591 6429-38.

592 WRIGHT, I. J., REICH, P. B., WESTOBY, M., ACKERLY, D. D., BARUCH, Z., BONGERS,
593 F., CAVENDER-BARES, J., CHAPIN, T., CORNELISSEN, J. H. C., DIEMER, M.,
594 FLEXAS, J., GARNIER, E., GROOM, P. K., GULIAS, J., HIKOSAKA, K., LAMONT,
595 B. B., LEE, T., LEE, W., LUSK, C., MIDGLEY, J. J., NAVAS, M. L., NIINEMETS, U.,
596 OLEKSYN, J., OSADA, N., POORTER, H., POOT, P., PRIOR, L., PYANKOV, V. I.,
597 ROUMET, C., THOMAS, S. C., TJOELKER, M. G., VENEKLAAS, E. J. & VILLAR, R.
598 2004. The worldwide leaf economics spectrum. *Nature*, 428, 821-827.

599 WU, Z., HUANG, S., ZHANG, X., WU, D., XIA, S. & LI, X. 2017. Regulation of plant immune
600 receptor accumulation through translational repression by a glycine-tyrosine-
601 phenylalanine (GYF) domain protein. *Elife*, 6.

602 ZHAI, J., JEONG, D. H., DE PAOLI, E., PARK, S., ROSEN, B. D., LI, Y., GONZALEZ, A. J.,
603 YAN, Z., KITTO, S. L., GRUSAK, M. A., JACKSON, S. A., STACEY, G., COOK, D.
604 R., GREEN, P. J., SHERRIER, D. J. & MEYERS, B. C. 2011. MicroRNAs as master
605 regulators of the plant NB-LRR defense gene family via the production of phased,
606 trans-acting siRNAs. *Genes Dev*, 25, 2540-53.

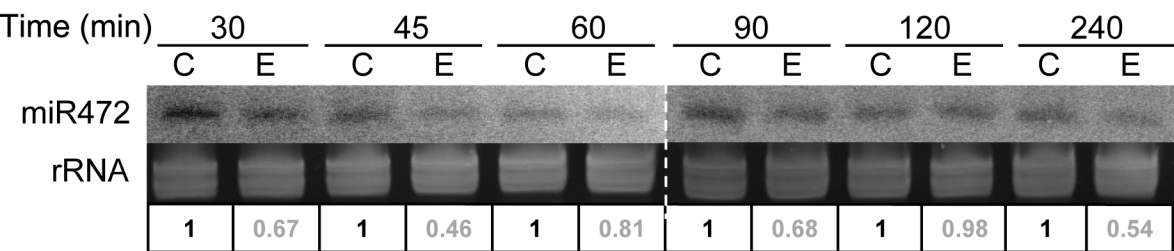
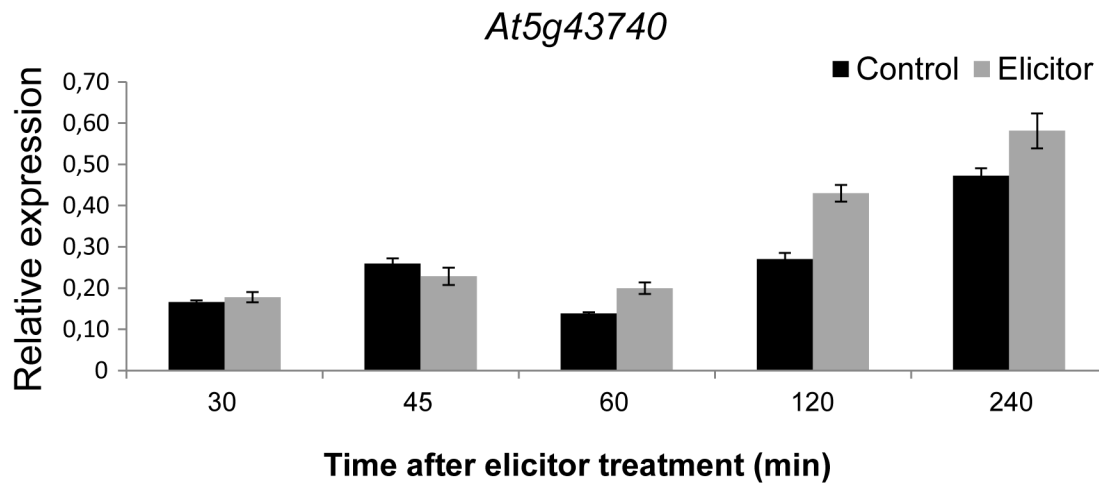
607 ZHANG, Y., XIA, R., KUANG, H. & MEYERS, B. C. 2016. The Diversification of Plant NBS-
608 LRR Defense Genes Directs the Evolution of MicroRNAs That Target Them. *Mol Biol
609 Evol*, 33, 2692-705.

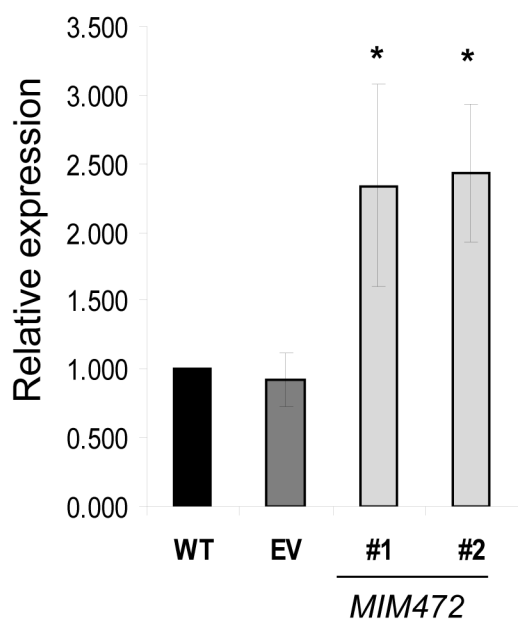
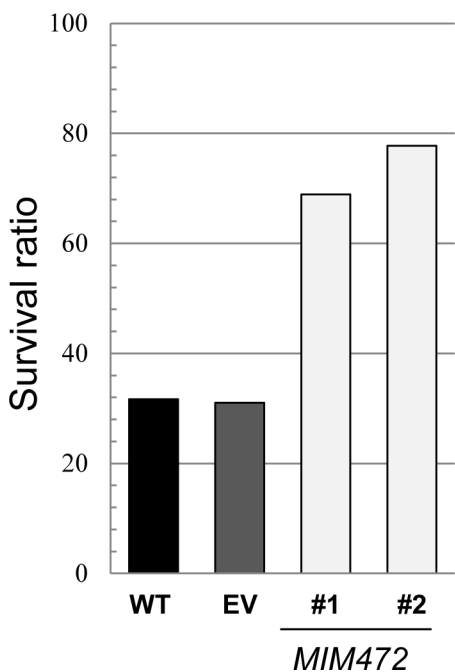
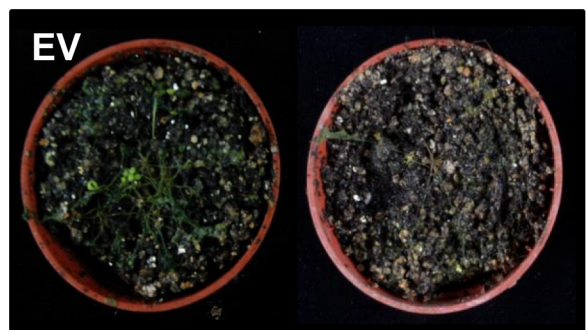
610 ZHU, C., LIU, J. H., ZHAO, J. H., LIU, T., CHEN, Y. Y., WANG, C. H., ZHANG, Z. H., GUO,
611 H. S. & DUAN, C. G. 2022. A fungal effector suppresses the nuclear export of AGO1-
612 miRNA complex to promote infection in plants. *Proc Natl Acad Sci U S A*, 119,
613 e2114583119.

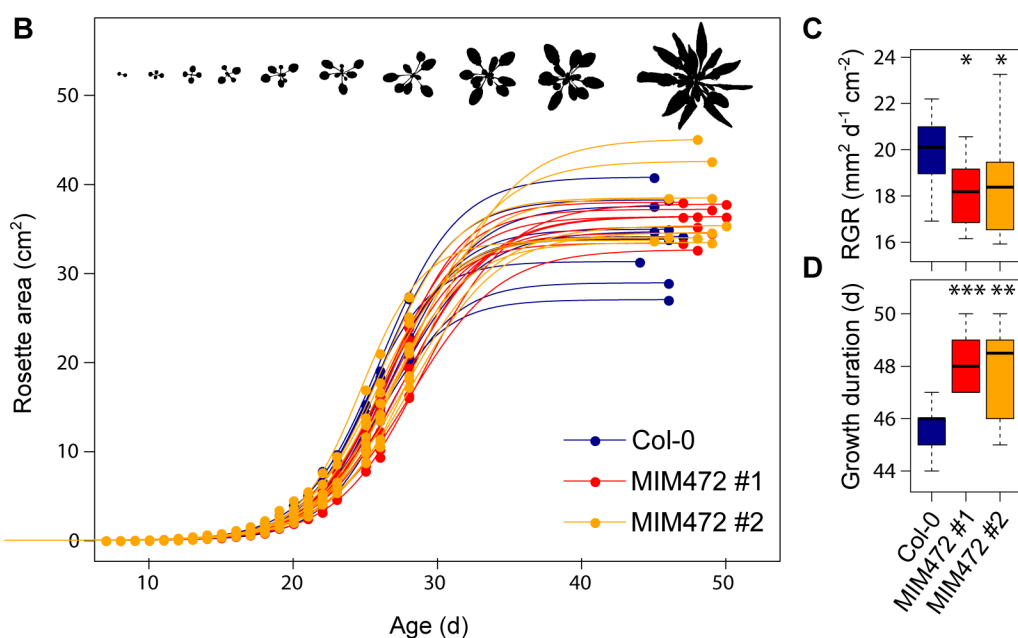
614 ZUST, T. & AGRAWAL, A. A. 2017. Trade-Offs Between Plant Growth and Defense Against
615 Insect Herbivory: An Emerging Mechanistic Synthesis. *Annu Rev Plant Biol*, 68, 513-
616 534.

617

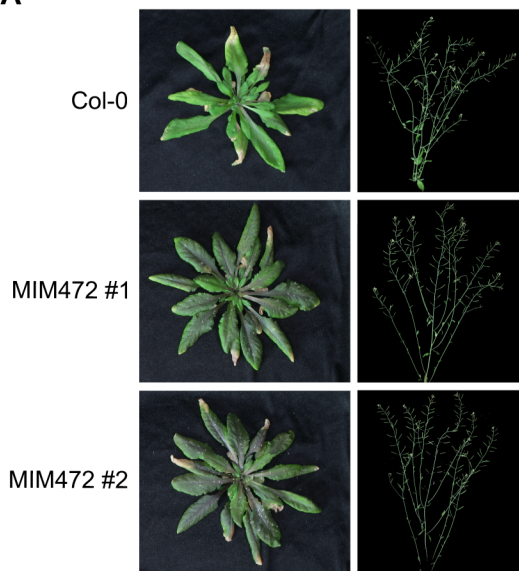
618

A**B**

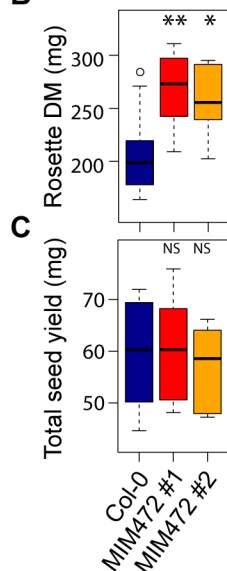
A*At5g43740***C****B**



A



B



C

Total seed yield (mg)

